FILOSE for Svenning

A Flow Sensing Bioinspired Robot

By Otar Akanyeti, Jennifer C. Brown, Lily D. Chambers, Hadi el Daou, Maria-Camilla Fiazza, Paolo Fiorini, Jaas Ježov, David S. Jung, Maarja Kruusmaa, Madis Listak, Andrew Liszewski, Jacqueline L. Maud, William M. Megill, Lorenzo Rossi, Antonio Qualtieri, Francesco Rizzi, Taavi Salumäe, Gert Toming, Roberto Venturelli, Francesco Visentin, and Massimo De Vittorio

The trend of biomimetic underwater robots has emerged as a search for an alternative to traditional propeller-driven underwater vehicles. The drive of this trend, as in any other areas of bioinspired and biomimetic robotics, is the belief that exploiting solutions that evolution has already optimized leads to more advanced technologies and devices. In underwater robotics, bioinspired design is expected to offer more energy-efficient, highly maneuverable,

Digital Object Identifier 10.1109/MRA.2014.2322287
Date of publication: 10 September 2014

agile, robust, and stable underwater robots. The 30,000 fish species have inspired roboticists to mimic tuna [1], rays [2], boxfish [3], eels [4], and others. The development of the first commercialized fish robot Ghostswimmer by Boston Engineering and the development of fish robots for field trials with specific applications in mind (http://www.roboshoal.com) mark a new degree of maturity of this engineering discipline after decades of laboratory trials.

So far, all fish robots have been equipped with off-the-shelf robotic sensors, such as cameras and sonars, whereas real fish have a dedicated sensing organ, the lateral line, for sensing flow. This sensing organ does not have a direct analogy in robotics. Neither do any of the human senses (e.g., smell and taste) have a direct counterpart to a flow sensor or even an English word for it (as there is for hearing or tasting). The word *svenning* was therefore proposed to describe flow sensing with the lateral line (in honor of Swedish biologist Sven Dijkgraaf [5]) [6]. Fish svenning is involved in a great variety of behaviors. Rheotactic behavior is navigation with respect to flow. Fish hold position or orient themselves toward or away from the current, and it is assumed that this behavior helps fish detect odors and food as well as possibly migrate upstream. Lateral line sensing helps fish catch prey by detecting the wake of a swimming fish [7]. It is also used in mediating schooling behavior and possibly helps with building cognitive flow maps. Tropomorphism (the reaction of the fish to flow stimuli) is common to all fish species [7].

All fish species and many sea mammals have flow-sensitive organs, but no underwater robot so far has made use of local flow sensing. Such an obvious discrepancy has inspired several research groups to develop artificial lateral line sensors [8] using different, often bioinspired, working principles. In [9], hot-wire anemometry-based flow sensors are used to detect a trail in still water left by a vibrating object (a so-called dipole source). A strongly bioinspired artificial flow sensor for flow speed detection is described in [10]. Whereas these artificial lateral line sensors are sensitive to flow speed (cantilever structures bending in flow), the sensors used to detect and identify the flow signatures of objects in [11] are pressure sensitive.

Traditionally, underwater robotics regards flow as a disturbance to be compensated by a vehicle's control algorithms. At the same time, biological evidence suggests that the ability to detect hydrodynamic events makes it possible to take advantage of the flow. An example is fishes' behavior in the periodic wake of a bluff object, where fish have been observed favoring certain hydrodynamically distinct locations. Fish swimming in those locations tire less quickly than those swimming in the steady flow. There are two behaviors that fish can exploit to reduce energy consumption in periodic turbulence. The first is the so-called Kármán gaiting, where fish adjust their tail beat frequency to the vortex shedding frequency of the object so that they can almost passively interact with the vortices. The second is the so-called flow refuging, where fish seek shelter in the object's hydrodynamic shadow in the reduced flow zone [12].

None of the underwater vehicles developed so far are capable of controlling themselves with respect to flow. Here we describe, to the best of our knowledge, the design of the first flow-sensitive underwater robot capable of flow-aided control. This article is an overview of the project Fish Locomotion and Sensing (FILOSE). It describes the research methodology, summarizes the main findings, and discusses and interprets the results of the project and the bioinspired approach.

Method of Bioinspired Robot Design

The general goal of the FILOSE project was to understand how fish sense flow and react to the flow stimuli, extract the underlying principles of this interaction, and then build robots with minimal complexity that react to the flow in the same way.

According to a classification by [13], the FILOSE project used a solution-driven approach to bioinspired design. We first indentified an interesting biological phenomenon: fish interaction with the flow and its implication for fish energy consumption. We then identified two core principles that led to robust and energy-efficient behavior in flow.

1) Fish have flow-sensitive organs that can perceive flow information. This led to the design of flow-sensitive sensor systems.
2) Fish have compliant bodies that make it possible to adjust their motion in vortices and use the environment to facilitate motion. This led to the design of a compliant soft-bodied robot.

The biological data were obtained from both the biology literature and experiments. The model animal used for the biological experiments was a rainbow trout. Fish behavior was recorded in a controlled hydrodynamic environment with a high-speed video camera and a digital particle image velocimetry (DPIV) system (Figure 1). Various flow conditions were investigated to measure the response of animals to variations in the sizes and strengths of wakes. The DPIV data and fish motion were later analyzed with the specially developed MathWorks freeware (http://www.mathworks.com/matlabcentral/fileexchange/37323).

An additional constraint posed to the bioinspired solution was the application of a reductionist approach: flow-relative behavior of an underwater robot with a minimal complexity of its mechanical design, sensor design, and control.

As is usually the case for research and development projects, the robot prototypes underwent several development stages in a frequent testing and developing cycle. The project also developed two alternative lateral line systems, only one of which was eventually tested onboard a moving robot.

Fish Robot Actuation

The underlying principle of the FILOSE mechanical design was the exploitation of the shape and material properties of the body to create mechanically simple but energetically favorable and robust robots. As such, we explored the extendibility of the soft robotics paradigm to underwater robotics. There are several successful examples of using the properties of soft materials to implement the principle of morphological computations—a design principle where the

design parameter space includes material properties and body geometry to reduce the system's complexity and increase robustness [14]. No underwater robots currently explicitly account for hydrodynamic effects to exploit the principles of morphological computation.

Direct application of a bioinspired design would imply replicating the highly distributed system of muscle fibers, which, with a current technology of electromechanical (EM) devices, would lead to large and complicated machines. Currently, the undulating motion of fish robots is achieved using serial chain kinematics of a caudal tail consisting of rigid links and rotational joints [1]–[4]. Those design approaches would contradict with our first identified design principle: using a soft and compliant body to facilitate interaction with flow. An alternative approach was first explored in [15], where the undulating motion was created with a soft body and a single motor. This article uses these findings and designs to build a bioinspired fish robot driven by a compliant part with some modifications to the mechanical design.

From a modeling point of view, a system with flexible links has infinite degrees of freedom. Unlike multibody rigid systems, exact solutions for modeling the dynamics are not feasible, so numerical methods are used instead. We extended the approach in [15] for modeling a nonhomogeneous body with the assumed modes method to derive the equations of motion. In contrast to [15] and [16], the modeling objectives are different: the model in [15] and [16] was developed to mimic the deformation of fish tails by taking the fish motion as an input and the torque amplitude as an output. In this article, the assumed method is used to derive the relationship between the applied forces/moments and the resulting deformations. Our model predicted, in accordance with the theory of vibration, that a compliant body exited by an external force can deform in defined modes that are dependent on its actuation and natural frequencies. The use of a rigid plate for actuation and the effects of internal damping are considered. Lighthill's elongated body theory is used to model the interaction between the robot and the surrounding water [17]. When mimicking the geometry, stiffness, and stiffness distribution of a rainbow trout, the kinematics of the fish can be achieved when the tail is actuated only by a single servo motor [18]. This is consistent with biological findings suggesting that, at the cruising speeds of 1–2 body length per second (BL/s), a fish uses mainly the anterior muscles of its body while the rest of the tail is passive and functions as a carrier of the traveling wave [19]. Our experiments showed good agreement between the predicted and measured motions [17]. They also demonstrated that such a system, as expected, was most efficient when actuated at its natural frequencies. We, therefore, further adopted a control mechanism where the tail beat frequency was fixed and the swimming speed of the robot was controlled by changing the tail beat amplitude. Another option would be to vary the stiffness of the tail, which is currently left for future work. Biological evidence also shows that fish change their swimming speed by controlling the frequency, actuation amplitude, and body stiffness [20]. Thus,

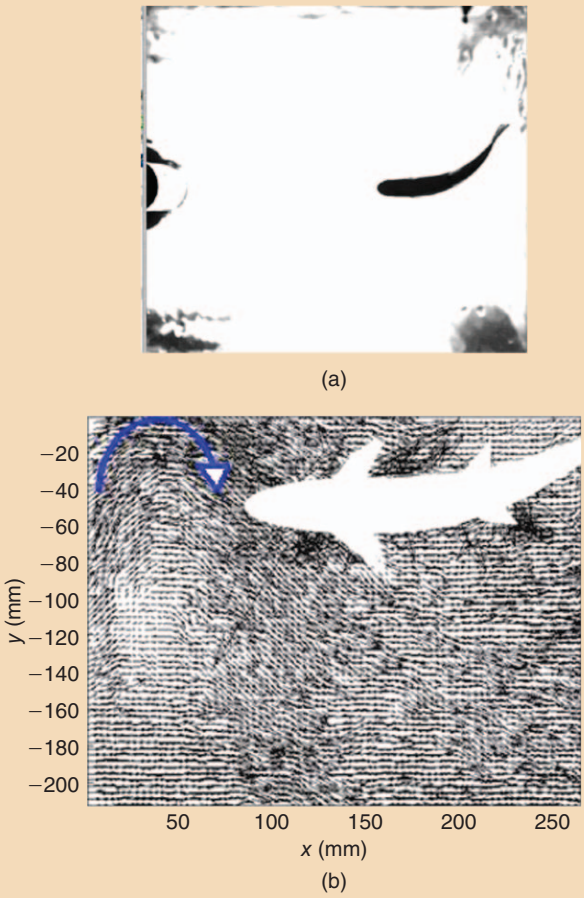

Figure 1. (a) A snapshot of a high-speed overview camera used to detect fish motion in a Kármán vortex street (KVS). A cylinder, partially visible on the left edge, is used to create periodic turbulence. (b) A DPIV image of the flow around a fish postprocessed to obtain the velocity vector field around the fish. The blue arrow indicates a vortex approaching the fish.

our simulations and experiments have implications for the soft-bodied robot design, showing that the kinematic envelope of a real fish is not always possible to achieve if the elasticity profile of the robot is static. The general theoretical framework developed for modeling a nonhomogeneous fin propulsor is, in the future, also suitable for analyzing the swimming modes of a swimmer with a stiffness control. A FILOSE robot prototype is shown in Figure 2, and its specifications are listed in Table 1. It consists of a rigid head and a compliant tail actuated by a servomotor that pulls two steel cables of an actuation plate. Flow sensors are mounted on the rigid head. Onboard data acquisition and servomotor control are implemented with an ARM processor with a Linux kernel. Flow sensing is analyzed in two dimensions, and, therefore, the robot has no buoyancy control. It is operated in a tethered mode to permit run-time debugging and data analysis.

Lateral Line Sensing

The sensing unit of a fish's lateral line is the neuromast, a hair cell that bends in the flow. The lateral line is a dual system

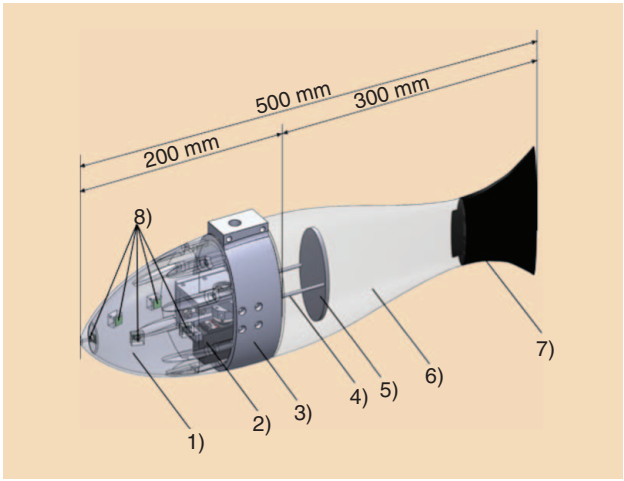

Figure 2. The FILOSE robot prototype. 1) Rigid head of the robot. 2) Servo-motor. 3) Middle section. 4) Steel cables. 5) Actuation plate. 6) Compliant tail. 7) Rigid fin. 8) Pressure sensors.

consisting of superficial and canal subsystems. Superficial neuromasts react to the flow speed on the surface of the fish's skin. Canal neuromasts are situated in the canals under the skin, and each of them measures the pressure difference between adjacent points where the canal emerges at the surface of the skin. This project has created several variations of two types of lateral line systems. The first type is based on microelectromechanical system (MEMS) stress-driven nitride-based bilayer design (Figure 3), equipped by a strain gauge. It consists of a multilayered cantilever beam, whose stress gradient along its cross section allows it to bend upward, mimicking a natural single hair cell of a neuromast in its EM characteristics and in its shape. Waterproofing is achieved by Parylene conformal coating. This Parylene encapsulation was demonstrated to be an efficient method to control the mechanical and sensory properties of a bioinspired artificial hair cell in a similar way as the natural hair cell [21]. The MEMS architecture easily adapts to flow variations due to its deformability in all points along the cantilever beam and shows robustness up to 1 BL/s. These lateral line sensors have been demonstrated to respond to flow fluctuations in the air and water but have not yet been demonstrated on an underwater robot.

Table 1. The FILOSE robot design specifications.

Length	0.5 m
Maximum width	0.085 m
Maximum height	0.156 m
Weight	3.04 kg
Motor	Futaba BLS152 brushless servo
Maximum torque	3 Nm
Controller	400-MHz ARM
Power source	External 24 V
Tail material	Dragon Skin 20 + Slacker additive by Smooth On
Young's modulus	83 kPa
Density	1,080 kg/m^3

The other lateral line system consists of commercial pressure sensors, complemented by specialized acquisition electronics, to improve its sensitivity and accuracy (Figure 4). The sensors were mounted on the rigid head of the fish robot prototypes while the complexity of the sensor systems varied from a simple two-sensor system to a three-dimensional (3-D) lateral line consisting of 16 sensors. The two-sensor systems demonstrate two approaches to apply a biomimetic approach on a different level of abstraction. The first one (a MEMS cantilever-based lateral line) is an approach of more directly applying the biological analogy. It directly copies the sensor mechanics of a neuromast—an erect mechanical structure that bends in flow. Also, it has a similar height to a real superficial neuromast—just about the length to reach through the boundary layer.

The other system represents a bioinspired design on a more abstract level. At this level of the abstraction, the direct analogy to neuromasts does not matter and, in fact, is also not applied. Real fish do not have neuromasts that directly measure pressure; instead, the canal lateral line is realized by using flow-sensitive neuromasts embedded into a canal system. In contrast, our system uses sensors that measure absolute pressure, and this has no direct analogy in fish biology. As such, the bioinspired approach adopts the solution to the problem rather than a direct biological analogy [22]. In this case, the problem is more efficient control in flow and the solution is to use flow sensing.

Hydrodynamic Environments

Live fish as well as underwater field robots operate in complicated hydrodynamic environments with turbulence, currents, and waves. These environments are too complicated to use as a testbed for a developing technology, and they are difficult to quantify and control. We, therefore, limited our problem to simply reproducible but still sufficiently complex and variable environments of periodic turbulence. Periodic turbulence occurs behind bluff objects in flow at moderate Reynolds numbers. It is characterized by a distinct repeating pattern of swirling vortices, known as the KVS. On the one hand, KVS is a well-studied hydrodynamic effect that can be realized in laboratory conditions with high repeatability. On the other hand, it is also a sufficiently common natural phenomenon, appearing, for example, in rivers behind rocks or other objects obstructing the flow or in oceans on a global scale as gyres.

Under laboratory conditions, KVS is created in a flume where the stream is obstructed with a cylinder. A cylinder or half-cylinder creates a well-defined periodic wake, whose characteristics can be adjusted by changing the incoming laminar flow speed or the diameter of the cylinder. The turbulence patterns can be visualized using a DPIV system. The mean velocity field and its standard deviation, vorticity field, wake width, the location of the vortex formation point, vortex

shedding frequency, and wavelength are some of the features that can be extracted and visualized.

Figure 5(a) shows the schematic of the periodic turbulence together with the experimentally obtained DPIV image in Figure 5(b). Figure 5(c) and (d) shows postprocessed DPIV data that represents, respectively, the vorticity and the velocity values. In Figure 5(c), blue and red clearly show the street of opposite signed vortices. The velocity graph in Figure 5(d) shows the suction zone and the reduced flow zone behind the cylinder. The reduced flow zone is the energetically favorable place that fish have been observed to prefer.

Characterization of Hyrodynamic Environments and Detecting Hydrodynamic Events

To develop new control algorithms for our biomimetic robot, we first needed to analyze the hydrodynamic environments in which the robot was situated. The DPIV analysis of the flow field made it possible to visualize these environments globally from the observer's perspective, whereas the pressure recordings from the immersed platform provided a local picture of the flow from a situated perspective. This platform was static and attached on a force gauge, which gave information about the hydrodynamic forces acting on the platform [23]. The force measurements taken at different locations in the vortex streets showed that the magnitude of lateral forces (perpendicular to the flow stream) was significantly larger in vortex streets and the measurements were oscillating with the vortex shedding frequency. In contrast, the drag (force along the flow stream) was 42% less than the one measured in uniform flow. This drag reduction was mainly due to the shadowing effect of the cylinder. These measurements provided insights on what a mobile robot would experience in vortex streets.

By correlating pressure data with ground-truth DPIV data, we were able to identify distinct pressure cues that signaled interesting hydrodynamic events taking place around the robot. First, we identified vortex streets. The key feature that separates vortex streets from other flow regimes is the regular pattern of vortices in space and time [24]. This regularity was reflected in the pressure measurements and was identified through Fourier decomposition [24]. When the robot was in the vortex street, pressure readings from all of the sensors detected the vortex shedding frequency as the dominant frequency [Figure 6(a)]. The number of sensors having a consensus on the dominant frequency decreased gradually when the robot was systematically moved away from the vortex street. Besides analyzing absolute pressure measurements, we found it advantageous to compare pressure at different locations. For instance, the pressure difference between the nose and side sensors was distinct in vortex streets and uniform flows. In uniform flows, the pressure recordings from the nose sensor were higher than those from the side sensors, whereas, in vortex streets, the opposite was true [25] [Figure 6(b)]. When the robot was moved away from the vortex street laterally, the pressure difference between the nose and side sensors increased gradually with the distance and finally reached normal values observed in uniform flows. The direction of motion (moving to the right or left) was determined by comparing the pressure values between the two sides of the robot.

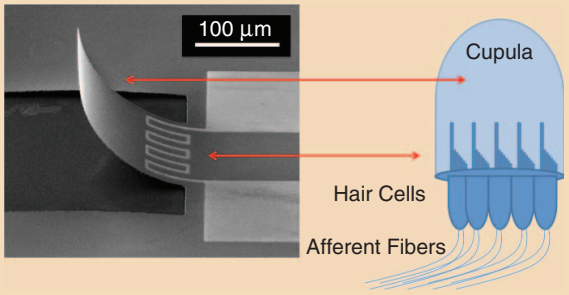

Figure 3. The bioinspired MEMS artificial lateral line flow sensor.

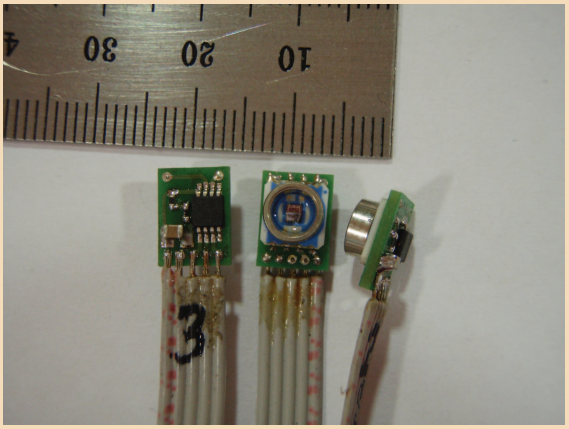

(a)

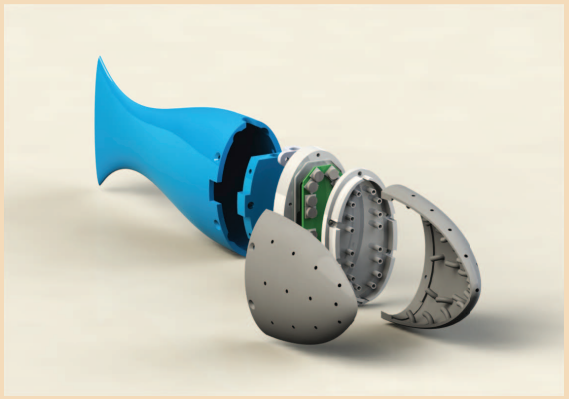

(b)

Figure 4. (a) The pressure sensors mounted on circuit boards with onboard electronics. The pressure sensors of an artificial lateral line use MS5407-AM diver's watch sensors by Intersema Sensoric SA. The sensing unit is connected as a Wheatstone bridge to give the sensor a high sensitivity of 56 mV/bar in the full scale (0–7 bar). We are using a 22-b differential analog-to-digital converter (ADC) with 124.5-mV reference voltage so that we can measure pressure with a least significant bit (LSB) of about (0.106 Pa). (b) The schematic of a fish robot prototype with a 3-D pressure-sensing lateral line.

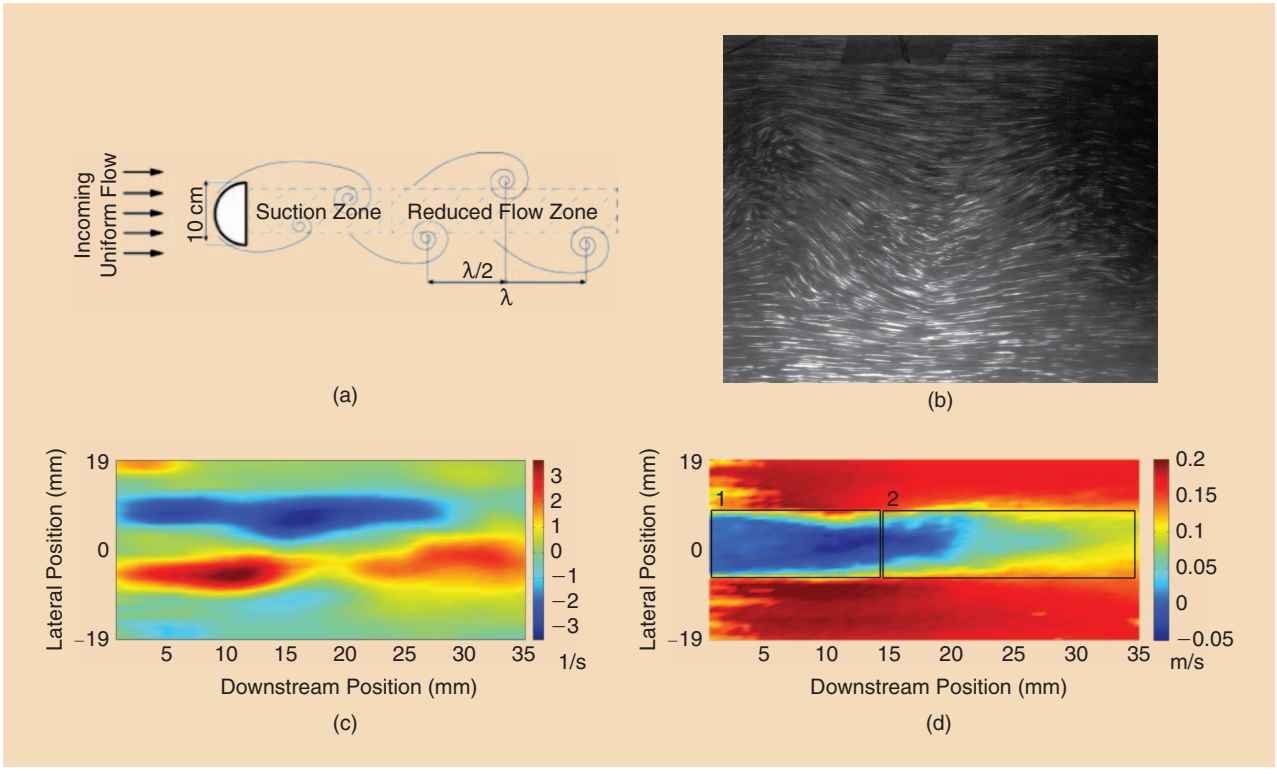

Figure 5. The KVS. (a) Schematics λ is the wavelength of the KVS. (b) A snapshot of a DPIV image of the flow obtained during fluid dynamics experiments. This data gets analyzed using (http://www.mathworks.com/matlabcentral/fileexchange/37323) and is an input for (c) and (d). (c) Instantaneous vorticity obtained from the DPIV image. The blue and red regions show high vorticity in opposite directions. The plot is obtained from two consequent DPIV snapshots, and a Gaussian filter is applied to smoothen the plot [25]. (d) Velocity readings averaged more than 10 s (500 frames obtained with 50-Hz frequency): 1) suction zone and 2) reduced flow zone.

After recognizing the presence of the vortex street, the next problem was to estimate the position and orientation of the robot with respect to the object's wake. The robot's distance from the cylinder was determined unambiguously by monitoring the turbulence intensity (calculated as the ratio of the standard deviation of the sensor readings to the mean value over an appropriate time window), and the amplitude of the dominant frequency [Figure 6(c)]. When the robot was moved closer to the suction zone, fewer sensors detected the vortex shedding frequency as the dominant frequency and the pressure at the tip of the robot was significantly lower. We found that the pressure difference between the left and right sensors was correlated with the orientation of the robot [Figure 6(d)].

Next, we extracted the robot's relative swimming velocity (i.e., flow velocity for a static robot) from the pressure measurements. In uniform flows, absolute pressure measurements as well as the pressure difference between the nose and side sensors increased quadratically with the flow velocity [24]–[26]. In vortex streets, we looked at the cross-correlation between sensor pairs randomly chosen from the same side of the robot. The peak values in the cross-correlation graphs indicated the amount of time required for a vortex to travel further down the body from one sensor to the next. The velocity of the vortex was then computed by dividing the distance between the two sensors to the estimated traveling time [27].

Up until now, our analysis was based on the pressure recordings obtained from a static robot configuration. To extract relevant flow information from the moving craft, we first need to understand how the pressure signals are impaired by the self-motion of the robot. For this purpose, we analyzed the motion of the robot in uniform flow by externally moving the robot with a robotic arm and recording pressure data and the robot's motion simultaneously. Two motion types were investigated: forward–backward motion along the direction of the flow and side-to-side motion perpendicular to the flow. We obtained two second-order polynomial models, which incorporated the position of the sensors, velocity, and acceleration of the robot to predict pressure distribution around the robot. The first model was presented in [26]. Through analysis of these models, we determined that, when the robot was moving with a velocity smaller than 0.2 BL/s, the self-motion effects on pressure sensing were negligible; the signal-to-noise ratio (the amplitude of pressure signals from hydrodynamic events divided by the amplitude of pressure signals generated by the self-motion of the robot) was adequate to characterize the hydrodynamic environments, as described in a static configuration. This method is also used to indentify parameters of the hydrodynamic environment in the section "Flow-Aided Control and Navigation" (Experiment 5) for flow-aided control. However, at higher

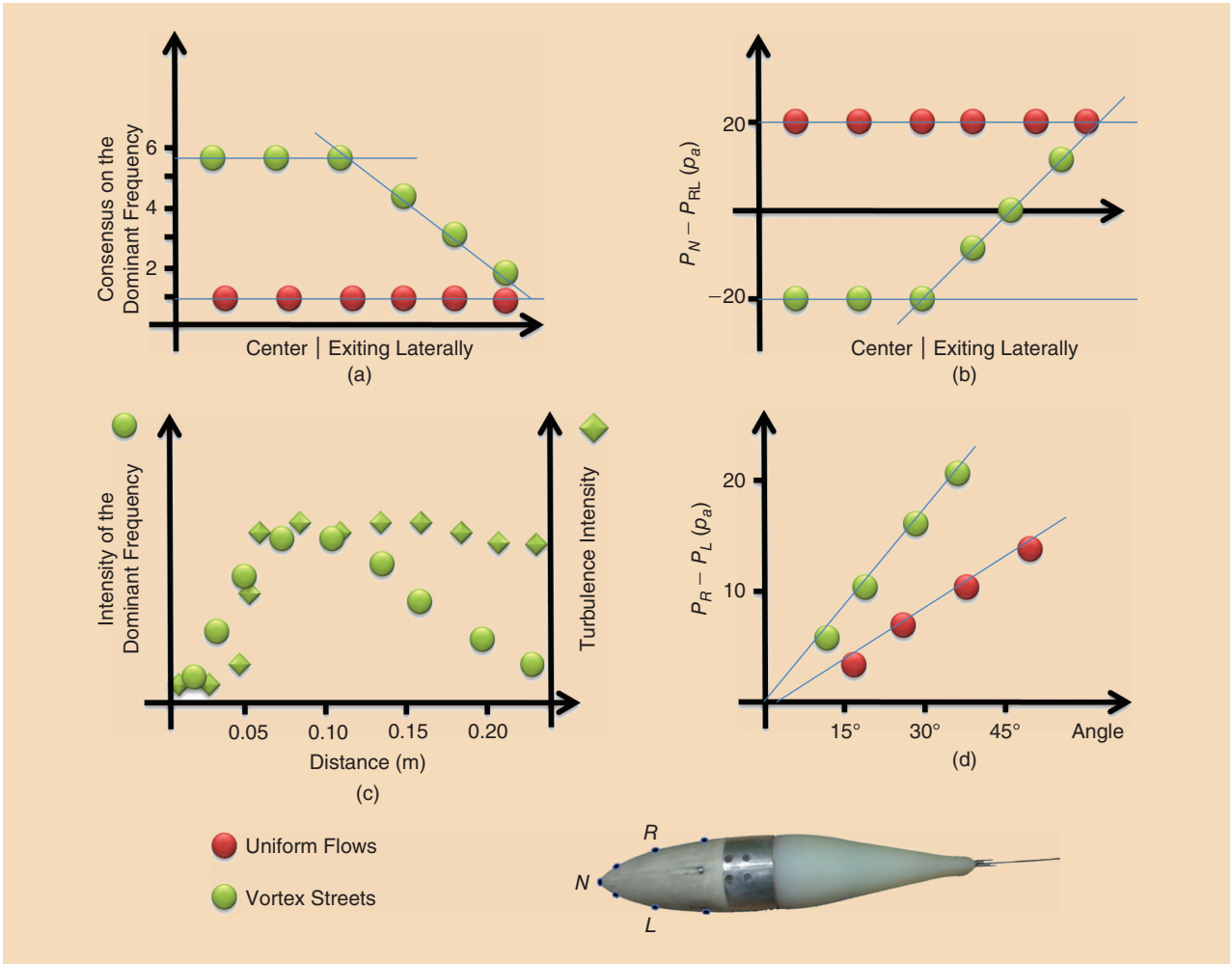

Figure 6. The pressure cues recorded from a robotic platform immersed in uniform flows (red-filled circle) and vortex streets (green-filled circle). (a) In vortex streets, most of the pressure signals were dominated by the vortex shedding frequency. The number of sensors detecting vortex shedding frequency decreased gradually when the robot was moved away from the vortex street. In contrast, in uniform flows, each pressure measurement had a different frequency with maximum amplitude, so there was no agreement among sensors. (b) The pressure difference between nose and side sensors is distinct between uniform flows and vortex streets. (c) Through an analysis of the turbulence intensity and amplitude of the dominant frequency, we were able to estimate the position of the robot with respect to the cylinder unambiguously. (d) The amplitude of the pressure difference between the right and left sides of the robot was linearly correlated to the robot's orientation with respect to the oncoming flow. The slope of the lines was different in uniform flows and vortex streets.

swimming velocities, the self-generated pressures would impair the perception of the environment. To minimize the self-motion effects, new filtering algorithms are needed so that external hydrodynamic events relevant to the robot's mission can be identified.

The robot's motion itself can be advantageous for sensing. For a stationary robot, the useful information has to be recovered from the analysis of a pressure pattern measured at one particular location. The moving robot can sample the hydrodynamic environment at multiple locations. By comparing multiple sensing patterns, it is possible to better evaluate the robot's current state. For instance, if the turbulence intensity and amplitude of the dominant frequency decrease as the robot moves from one arbitrary point to the next, we can deduce from Figure 6(c) that the robot would approach the cylinder. In Experiment 5, pressure gradients are used to guide the moving robots toward the control set point in the reduced flow zone.

Flow-Aided Control and Navigation

The experiments of flow-aided control of the FILOSE robot are conducted in uniform flow and in KVS in a flow tank, where the flow and the trajectories of the robot are recorded (Figure 7). The experimental setup is described in Figure 8. Experiments are conducted in a flow tunnel with a 0.5-m wide, 0.5-m high, and 1.5-m long working section. The robot is freely swimming but its motion is limited to two dimensions to permit trajectory tracking and motion analyses using an overview camera. The following experiments of flow-aided control were conducted.

Experiment 1: Detection of Flow Direction and Swimming Against the Flow

The direction of the uniform flow is detected by measuring the pressure difference between two sensors on the sides of the robot. A simple Braitenberg controller turns the robot

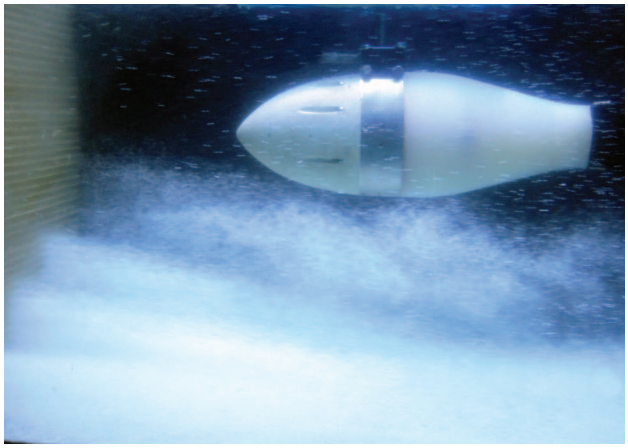

Figure 7. The FILOSE robot in flow in the DPIV flume pipe. The white dust is DPIV particles used to visualize the flow. A collimator, which is visible to the left, is used to create a uniform flow in the flow pipe. (Photo courtesy of the Centre of Biorobotics, Tallinn University of Technology.)

toward the side with a higher pressure by adding an offset to the tail actuation signal. In uniform flow, two sensors and a simple Braitenberg controller were demonstrated to be sufficient to keep the fish robot oriented into the flow [28]. Figure 9 demonstrates the trajectories of the robot with and without feedback control and those compared with feedback control with the overview camera.

Experiment 2: Flow-Aided Trajectory Following

The robot in uniform flow uses a sideslipping maneuver. Sideslipping permits the robot to move laterally with respect to the incoming flow by exploiting its passive dynamics. Sideslipping is controlled by adjusting the heading of the robot with respect to the flow when following a closed trajectory in a stream. A simple proportional-integral-derivative (PID) controller was implemented for controlling the motion of side slipping laterally and transversely [29]. Traditionally, when an underwater robot follows a trajectory, the coordinates of the waypoints are given in the global coordinates and also the speed of the robot is calculated with respect to Earth's reference frame. This experiment suggests that it is advantageous to know the flow-relative speed. It leads to reduced energy consumption and more stable trajectories. Figure 10(a) shows the trajectory of an underwater robot in the flow compared with the desired trajectory and the trajectory where the robot is not aware of the flow conditions (the standard case for underwater robot control). The average deviation from the desired trajectory is reduced by 3% for trajectory 1 (where the parallel flow disturbs the vehicle a little) and 82% for trajectory 2 where the flow is mostly perpendicular to the desired trajectory. Figure 10(b) shows a more complicated case of following a closed trajectory in the flow that the robot traverses without sharp turns in the waypoints.

Experiment 3: Station-Holding in a Steady Stream

The robot estimated the flow speed from the pressure readings at the sides of the head. The flow speed is calibrated with respect to the sensor readings at 0 m/s velocity. We used these signals as short-term odometry to compensate for the downstream drift using a PID controller. Our experiments using the setup in Figure 8 showed that the odometry reading from pressure sensors estimated the robot's relative position with respect to the flow, with an accuracy less than one body length of the robot over a duration of 270 s with varying flow speeds. (The initial flow speed was 11 cm/s and it was increased after every 30 s by 1 cm/s up to 19 cm/s.) The

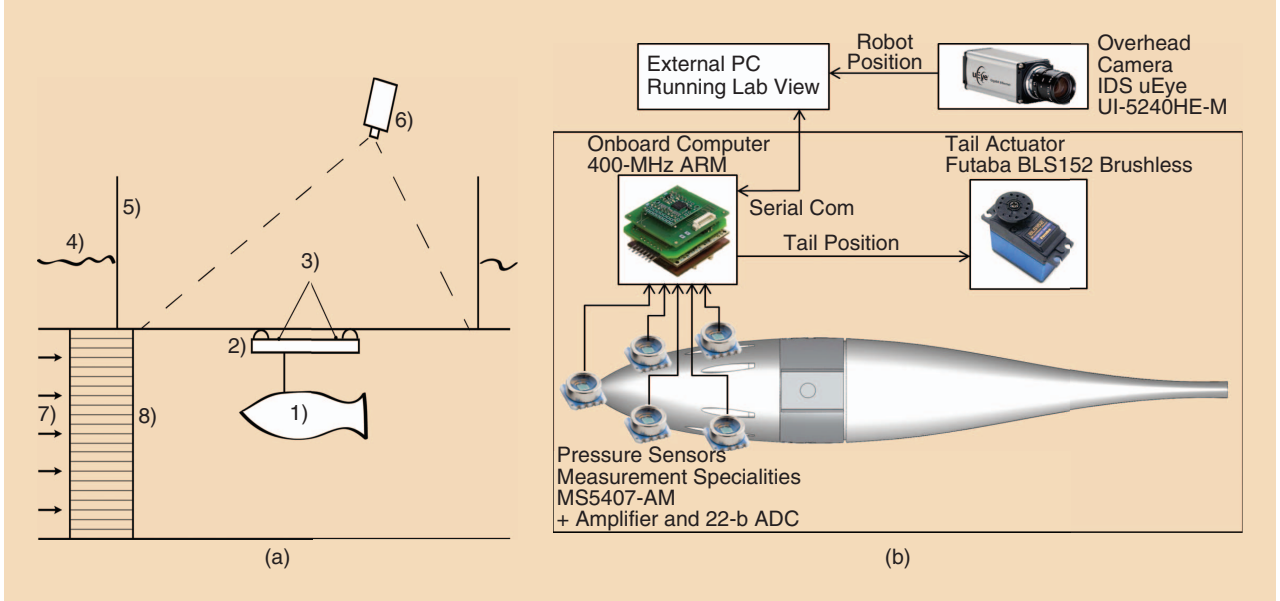

Figure 8. (a) The experimental setup [25] and side view of the flow tunnel. 1) Robotic fish. 2) Floater. 3) LEDs on the floater for position tracking. 4) Water level. 5) Transparent glass box on top of the tunnel for filming. 6) Camera for position tracking. 7) Flow direction. 8) Collimators. (b) Control schematics of the robot and the experiment.

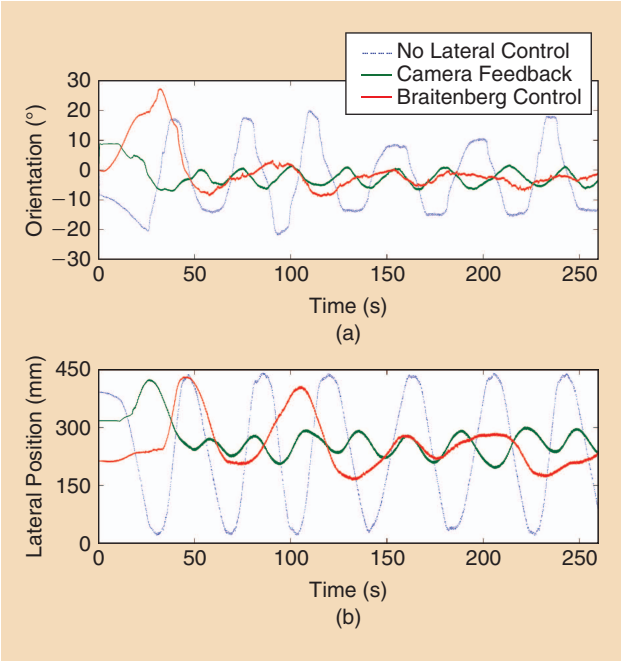

Figure 9. (a) The orientation and lateral displacement of the robot recorded with an overview camera [25]. (b) The robot is held in its longitudinal position with the feedback control from the camera for recording while the orientation is controlled by the Braitenberg controller using flow sensors or by the camera (for comparison). With no heading control, the robot is bouncing between the flow tank's walls (blue line) while the precision of the heading control based on flow sensing (red) and camera feedback (green) are almost comparable.

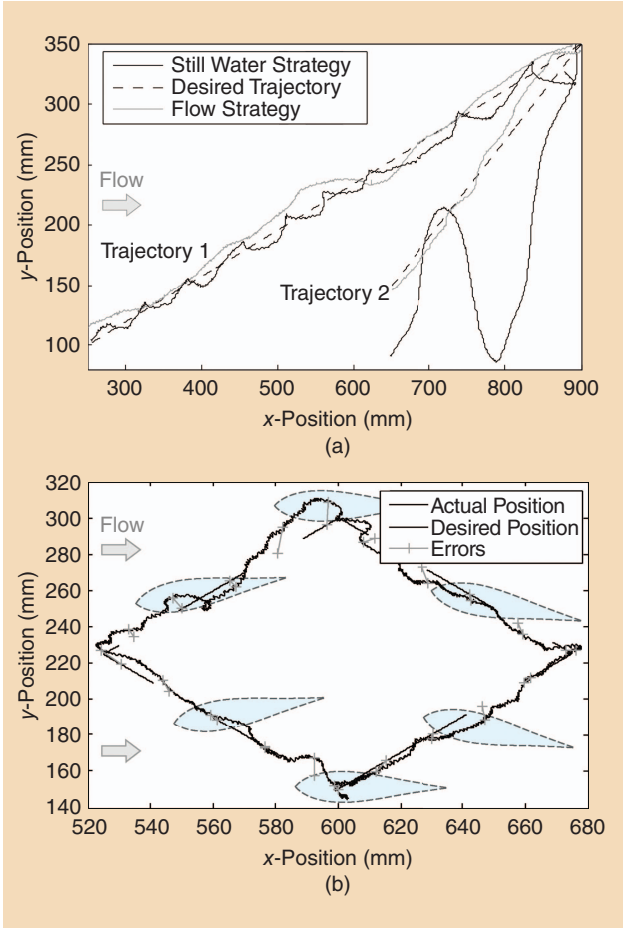

Figure 10. A flow-aided trajectory following [29]. (a) A straight line in the flow (dashed line) using the sideslipping maneuver and flow information (thin line) and without flow information (thick line). (b) A closed trajectory in the flow. Laminar flow is directed from left to right, and the robot's pose in the flow is marked in light blue.

downstream drift at the end of the experiment was 1/5 of the robot's body length [25]. Currently, a standard method in underwater robotics is to use an acoustic Doppler current profiler (ADCP) to estimate the bulk flow speed. ADCPs are bulky, costly, and energy-consuming devices that are not suitable for small underwater vehicles. The lateral-line-based odometry can here provide a low-cost alternative for estimating the flow-relative speed and providing the velocity estimate in the absence of a global reference.

Experiment 4: Reducing Energy Consumption in Turbulence by Exploiting Vorticity

The experimental setup of this experiment is different than that shown in Figure 8 in that the robot is harnessed to a force plate for force measurements. The lateral line signals are used to control the tail beat timing. A motion pattern similar to Kármán gaiting is achieved by adjusting the frequency of the tail beat to the vortex shedding frequency and fine-tuning the tail beat timing. The tail bends against the high-pressure zone created by the vortex, and the robot takes advantage of the increased perpendicular component of the lift force created by pressure differences on both sides of the flexing tail (Figure 11). The results are compared with those of the tail fin propulsion in the steady flow with the same incoming flow speed. In comparison, 100% more thrust is created in KVS with the appropriate tail beat timing than in steady flow [30].

Experiment 5: Reducing Energy Consumption by Holding Station in a Hydrodynamic Shadow

We first identified the reduced flow zone [zone 2 in Figure 5(d)] behind the object from DPIV images and adjusted the thresholds of pressure readings to identify the point of reference for station-holding. The robot compensates for the lateral and longitudinal drift using PID controllers and keeping the station in the hydrodynamic shadow. Monitoring the motor current consumption reveals that swimming in the reduced flow zone consumes 7% less energy behind the cylindrical object. The standard deviation of the downstream position behind the cylinder is 40.5 mm, and that of the lateral position is 12.7 mm. When the cylinder was replaced by the cuboid, creating a sharper pressure drop between the suction zone and the reduced flow zone, the energy consumption reduced by 17%. The standard deviation of the downstream position was 21.2 mm, and that of the lateral position was 13.3 mm in this experiment. The duration of both experiments was 270 s [25]. The trajectories of the robots are plotted in Figure 12.

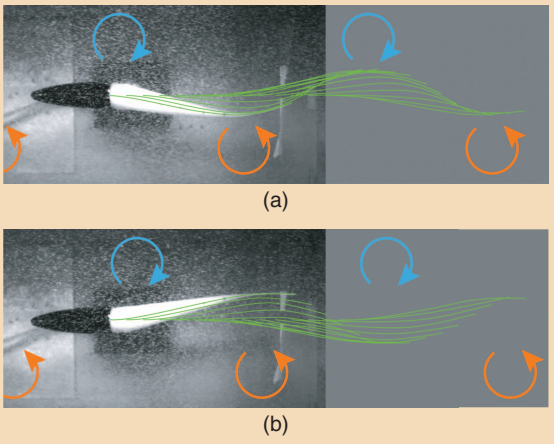

Figure 11. The fish tail position with respect to the vortex when the craft produces (a) max thrust and (b) minimal thrust.

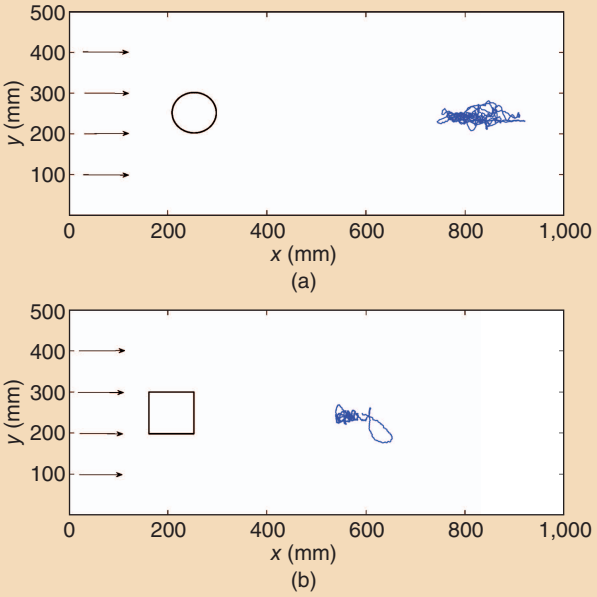

Figure 12. The center of mass trajectory of a robotic fish over 270 s in a reduced flow zone [Zone 2 in Figure 5(d)] generated by the (a) cylinder and (b) cuboid with the experimental setup in Figure 8 [25].

Experiment 6: Comparative Experiments

Trajectories of a real fish and the robot were recorded in a uniform flow and when swimming behind in an object's wake. A swim path analysis to determine path tortuosity (as a measure of the complexity of the trajectory) was performed on data extracted from high-speed video recordings of four rainbow trout (*Oncorhynchus mykiss*) with a total body length (L) of 18 ± 3 cm swimming. Two different points on the fish midlines were used to track the path at 10 and 30% body length points, in flow speeds of 10, 20, and 30 cm/s and behind a range of cylinders with diameters of 2.5, 4.5, and 10 cm.

All fish species and many sea mammals have flow-sensitive organs, but no underwater robot so far has made use of local flow sensing.

Path tortuosity was determined from the fractal dimension or fractal d, one of a number of possible tortuosity estimators. Path analysis using the fractal dimension (D) data (estimated by the dividers method to determine the path length at varying step sizes) indicates that trout swimming in the unsteady KVS had a significantly lower path tortuosity than the steady uniform flow ($P < 0.05, n = 45$). Within the KVS environment, the path tortuosity of the largest-cylinder-diameter swim paths was significantly lower than that of the smaller cylinder diameters ($P < 0.05, n = 45$). A similar decrease in path tortuosity was measured when comparing the robot's trajectories in uniform flow and behind the cylinder.

This suggests that the path tortuosity is influenced by the hydrodynamic forces in the environment. Fish and robots in KVS appear to have smoother trajectories than those in uniform flow. We hypothesize that the hydrodynamic forces within the KVS drive the fish/robot toward the center of the wake and thereby reduce the complexity of the trajectories, whereas, in the steady flow, the environment has no such environmental cues that help to stabilize the fish or the robot. This explanation is supported by measurements in [23], where we show that the drag profile in KVS has a single local minimum at the midline of the wake.

Discussion

Though all 30,000 fish species have a lateral line organ, so far, there have been no technological counterparts to lateral line sensing in use for controlling underwater robots. The contribution of this article is to give a new sense, svenning, to aid the control of underwater vehicles. Once flow can be perceived, it can be analyzed and exploited for a variety of purposes. Traditionally, flow is treated as a disturbance in underwater robotics, to be compensated by the vehicle's control algorithms. With flow sensing, flow becomes a source of information, and, with clever sensing–actuation coupling, flow becomes a source of energy. Flow information can be fused with other sensor modalities and used for vehicle control. Knowing flow direction and strength permits movement with respect to the flow-relative reference frame as opposed to the global reference frame.

Flow information can also be incorporated into higher-level behaviors. Salient flow features, such as wakes of objects or steady currents, could be identified and classified and used as landmarks. Again, this information can be fed into a vehicle's navigation algorithm and used for map building and localization. Flow sensing permits identification of flow conditions where a vehicle's control is more stable and energy efficient. Coupling of flow sensing and actuation opens up

new opportunities to exploit flow for energy-efficient motion. Flow-relative control could also make traditional rigid hull underwater robots more efficient, but there is more to gain from flow perception and robot–fluid interaction from small devices, with flexible fins or rudders.

This aligns flow-sensing robots with the increasingly popular trend of soft robotics. Hydrodynamic forces can be best exploited if the craft is continuous, flexible, and able to vary its stiffness to adapt to different conditions. For example, our FILOSE robot would need a stiffer tail to produce enough thrust in uniform flow and a floppy passive tail to bend in KVS between the vortices. Designing such a robot can be a challenging problem for mechanical engineering. Moreover, we still have a limited understanding of the theoretical foundations of coupled compliant body-fluid motion; the hydrodynamic effects in turbulence are complex and highly nonlinear and do not lend themselves well to real-time control. Our work shows that, in many cases, approximate linear control laws are sufficient, but it is unclear as to how well they scale up to more complicated tasks and environments.

Another challenge is to develop suitable lateral line sensors that would tremendously improve the perception and analysis of the fluid environment. Although several promising solutions exist, the FILOSE robot is the first one to exploit the lateral line sensors onboard a moving craft. The project developed in parallel two sensing systems, one based on MEMS technology and direct biological analogy, and another based on the commercial sensors and functional similarity. The first system was more complicated, and improving its reliability for onboard control is still an ongoing work. The other system was successfully demonstrated for control of the robot. However, its sensitivity does not compare with the one of the biological systems and may not be sufficient for complex real-world environments. For comparison, the sensitivity of fish canal lateral line neuromasts is four orders of magnitude higher than that of the FILOSE pressure sensors, which inevitably sets a limit to what the svenning robot can perceive compared with fish [31]. From the point of view of bioinspired design methodology, conclusions can be drawn for designing bioinspired robots in the future. The success of biologically inspired design critically depends on establishing an analogy at the appropriate level of abstraction [22]. This was well evident from comparing the application of two different flow-sensing systems as well as the design of the compliant tail, where functional similarity was preferred over a direct analogy of a real-fish highly distributed actuation system. Finally, the bioinspired locomotion and lateral line sensing offer possibilities to better understand how real fish sense the world and react to hydrodynamic stimuli and to use those findings to build better technology on the next development iteration. From the experiments conducted with the robot, we know what the flow looks like from the situated perspective and what information is there to sense. We also understand from comparative experiments as to how the stability and efficiency of the robot or a fish arise from the interplay with the environmental conditions. If a rigid methodology is used to conduct comparative experiments with fish and robots, that will both enhance our understanding of nature and enable the development of better technology.

Acknowledgments

This work was financed by the European Commission 7th Framework program under FP7-ICT-2007-3 STREP project FILOSE. We would like to thank Prof. John Long from Vassar College and Prof. Thor I. Fossen from the Norwegian University of Science and Technology for their valuable feedback throughout the project.

References

[1] D. Barrett, M. Grosenbaugh, and M. Triantafyllou, "The optimal control of a flexible hull robotic undersea vehicle propelled by an oscillating foil," in *Proc. Symp. Autonomous Underwater Vehicle Technology*, 1996, pp. 1–9.

[2] K. H. Low, "Modelling and parametric study of modular undulating fin rays for fish robots," *Mech. Mach. Theory*, vol. 44, no. 3, pp. 615–632, 2009.

[3] P. Kodati, J. Hinkle, A. Winn, and X. Deng, "Microautonomous robotic ostraciiform (MARCO): Hydrodynamics, design, and fabrication," *IEEE Trans. Robot.*, vol. 24, no. 1, pp. 105–117, 2008.

[4] K. A. McIsaac and J. P. Ostrowski, "Experiments in closed-loop control for an underwater eel-like robot," in *Proc. IEEE Int. Conf. Robotics Automation*, 2002, vol. 1., pp. 750–755.

[5] S. van Netten, Private communication. Groningen, The Netherlands, Nov. 2012.

[6] S. Coombs, P. Görner, and H. Münz, *The Mechanosensory Lateral Line: Neurobiology and Evolution*. New York: Springer-Verlag, 1989.

[7] J. Mogdans and H. Bleckmann, "Coping with flow: Behavior, neurophysiology and modeling of the fish lateral line system," *Biol. Cybern.*, vol. 106, nos. 11–12, pp. 627–642, 2012.

[8] J. Tao and X. B. Yu, "Hair flow sensors: From bio-inspiration to bio-mimicking—A review," *Smart Mater. Struct.*, vol. 21, no. 11, p. 113001, 2012.

[9] Y. Yang, J. Chen, J. Engel, S. Pandya, N. Chen, C. Tucker, S. Coombs, D. L. Jones, and C. Liu, "Distant touch hydrodynamic imaging with an artificial lateral line," *Proc. Natl. Acad. Sci.*, vol. 103, no. 50, pp. 18891–18895, 2006.

[10] M. E. McConney, N. Chen, D. Lu, H. A. Hu, S. Coombs, C. Liub, and V. V. Tsukruk, "Biologically inspired design of hydrogel-capped hair sensors for enhanced underwater flow detection," *Soft Matter*, vol. 5, no. 2, pp. 292–295, 2009.

[11] V. I. Fernandez, A. Maertens, F. M. Yaul, J. Dahl, J. H. Lang, and M. S. Triantafyllou, "Lateral-line-inspired sensor arrays for navigation and object identification," *Mar. Technol. Soc. J.*, vol. 45, no. 4, pp. 130–146, 2011.

[12] J. Liao and A. Cotel, "Effects of turbulence on fish swimming in aquaculture," in *Swimming Physiology of Fish*, A. P. Palstra and J. V. Planas, Eds. Berlin Heidelberg, Germany: Springer-Verlag, 2013, pp. 109–127.

[13] M. Helms, S. Vattam, and A. K. Goel, "Biologically inspired design: Process and products," *Des. Stud.*, vol. 30, no. 5, pp. 606–622, 2009.

[14] R. Pfeifer, M. Lungarella, and F. Iida, "The challenges ahead for bioinspired 'soft' robotics," *Commun. ACM*, vol. 55, no. 11, pp. 76–87, 2012.

[15] B. P. Epps, P. Valdivia y Alvarado, K. Youcef-Toumi, and A. H. Techet, "Swimming performance of a biomimetic compliant fish-like robot," *Exp. Fluids*, vol. 47, no. 6, pp. 927–939, 2009.

[16] P. P. A. Valdivia y Alvarado, "Design of biomimetic compliant devices for locomotion in liquid environments," Ph.D. dissertation, Dept. Mech. Eng., Massachusetts Inst. Technol., Cambridge, MA, 2007.

[17] H. E. Daou, T. Salumäe, L. D. Chambers, W. M. Megill, and M. Kruusmaa, "Modelling of a biologically inspired robotic fish driven by compliant parts," *Bioinspir. Biomim.*, vol. 9, no. 1, p. 016010, 2014.

[18] T. Salumäe and M. Kruusmaa, "A flexible fin with bioinspired stiffness profile and geometry," *J. Bionic Eng.*, vol. 8, no. 4, pp. 418–428, 2011.

[19] L. G. John, J. H. Long, M. J. Mchenry, and N. C. Boetticher, "Undulatory swimming: How traveling waves are produced and modulated in sunfish (Lepomis gibbosus)," *J. Exp. Biol.*, vol. 192, no. 1, pp. 129–145, 1994.

[20] M. J. McHenry, C. A. Pell, and J. H. Long, Jr., "Mechanical control of swimming speed: Stiffness and axial wave form in an undulatory fish model," *J. Exp. Biol.*, vol. 198, pp. 2293–2305, Nov. 1995.

[21] F. Rizzi, A. Qualtieri, L. D. Chambers, W. M. Megillb, and M. de Vittorioac, "Parylene conformal coating encapsulation as a method for advanced tuning of mechanical properties of an artificial hair cell," *Soft Matter*, vol. 9, no. 9, pp. 2584–2588, 2013.

[22] J. Yen and M. Weissburg, "Perspectives on biologically inspired design: Introduction to the collected contributions," *Bioinspir. Biomim.*, vol. 2, no. 4, 2007.

[23] G. Toming, T. Salumae, A. Ristolainen, F. Visentin, O. Akanyeti, and M. Kruusmaa, "Fluid dynamics experiments with a passive robot in regular turbulence," in *Proc. IEEE Int. Conf. Robotics Biomimetics*, 2012, pp. 532–537.

[24] O. Akanyeti, R. Venturelli, F. Visentin, L. Chambers, W. M. Megill, and P. Fiorini, "What information do Kármán streets offer to flow sensing?" *Bioinspir. Biomim.*, vol. 6, no. 3, p. 036001, 2011.

[25] T. Salumäe and M. Kruusmaa, "Flow-relative control of an underwater robot," *Proc. Royal Soc. A: Math. Phys. Eng. Sci.*, vol. 469, no. 2153, pp. 20120671–20120671, 2013.

[26] O. Akanyeti, L. D. Chambers, J. Ježov, J. Brown, R. Venturelli, M. Kruusmaa, W. M. Megill, and P. Fiorini, "Self-motion effects on hydrodynamic pressure sensing: Part I. Forward–backward motion," *Bioinspir. Biomim.*, vol. 8, no. 2, p. 026001, 2013.

[27] R. Venturelli, O. Akanyeti, F. Visentin, J. Ježov, L. D. Chambers, and G. Toming, "Hydrodynamic pressure sensing with an artificial lateral line in steady and unsteady flows," *Bioinspir. Biomim.*, vol. 7, no. 3, p. 036004, 2012.

[28] T. Salumae, I. Rano, O. Akanyeti, and M. Kruusmaa, "Against the flow: A Braitenberg controller for a fish robot," in *Proc. IEEE Int. Conf. Robotics Automation*, 2012, pp. 4210–4215.

[29] D. Jung, P. Pott, T. Salumäe, and M. Kruusmaa, "Flow-aided trajectory following of an underwater robot," in *Proc. IEEE Int. Conf. Robotics Automation*, 2013, pp. 4602–4607.

[30] J. Jezov, O. Akanyeti, L. D. Chambers, and M. Kruusmaa, "Sensing oscillations in unsteady flow for better robotic swimming efficiency," in *Proc. IEEE Int. Conf. Systems, Man Cybernetics*, 2012, pp. 91–96.

[31] S. Netten, "Hydrodynamic detection by cupulae in a lateral line canal: Functional relations between physics and physiology," *Biol. Cybern.*, vol. 94, no. 1, pp. 67–85, 2006.

Otar Akanyeti, University of Verona, Italy (now with University of Florida, Gainesville). E-mail: otar@whitney.ufl.edu.

Jennifer C. Brown, University of Bath, United Kingdom. E-mail: j.c.brown@bath.ac.uk.

Lily D. Chambers, University of Bath, United Kingdom (now with University of Bristol, United Kingdom). E-mail: L.Chambers@bristol.ac.uk.

Hadi el Daou, Centre for Biorobotics, Tallinn University of Technology, Estonia (now with Imperial College London, United Kingdom). E-mail: hadi.eldaou@gmail.com.

Maria-Camilla Fiazza, University of Verona, Italy. E-mail: tokhami@gmail.com.

Paolo Fiorini, University of Verona, Italy. E-mail: paolo.fiorini@univr.it.

Jaas Ježov, Centre for Biorobotics, Tallinn University of Technology, Estonia. E-mail: jaas.jezov@ttu.ee.

David S. Jung, Centre for Biorobotics, Tallinn University of Technology (now with University of Nottingham, United Kingdom). E-mail: david.s.jung@web.de.

Maarja Kruusmaa, Centre for Biorobotics, Tallinn University of Technology, Estonia. E-mail: Maarja.Kruusmaa@ttu.ee.

Madis Listak, Marine Systems Institute, Tallinn University of Technology, Estonia. E-mail: Madis.Listak@ttu.ee.

Andrew Liszewski, University of Bath, United Kingdom. E-mail: andyliszewski@gmail.com.

Jacqueline L. Maud, Plymouth Marine Laboratory, United Kingdom (now with Plymouth Marine Laboratory). E-mail: jama@pml.ac.uk.

William M. Megill, University of Bath, United Kingdom (now with Rhine-Waal University of Applied Sciences, Germany). E-mail: william.megill@hsrw.eu.

Lorenzo Rossi, Italian Institute of Technology. E-mail: lorenzo.rossi@iit.it.

Antonio Qualtieri, Center for Bio-Molecular Nanotechnologies, Italian Institute of Technology. E-mail: antonio.qualtieri@iit.it.

Francesco Rizzi, Center for Bio-Molecular Nanotechnologies, Italian Institute of Technology. E-mail: francesco.rizzi@iit.it.

Taavi Salumäe, Centre for Biorobotics Tallinn University of Technology, Estonia. E-mail: Taavi.Salumäe@ttu.ee.

Gert Toming, Centre for Biorobotics Tallinn University of Technology, Estonia. E-mail: Gert.Toming@ttu.ee.

Roberto Venturelli, University of Verona, Italy. E-mail: venturelli.roberto@gmail.com.

Francesco Visentin, University of Verona, Italy. E-mail: francesco.visentin@univr.it.

Massimo De Vittorio, University of Salento and Italian Institute of Technology, Italy. E-mail: massimo.devittorio@unisalento.it.